

Thermal atoms facilitate intensity clipping between vectorial dual-beam generated by a single metasurface chip

Chen Qing, Jialong Cui, Lishuang Feng, and Dengke Zhang

*School of Instrumentation and Optoelectronic Engineering, Beihang University, Beijing 100191, China and
Email: dkzhang@buaa.edu.cn*

Manipulating vector beams is pivotal in fields such as particle manipulation, image processing, and quantum communication. Flexibly adjusting the intensity distribution of these beams is crucial for effectively realizing these applications. This study introduces a vectorial dual-beam system utilizing thermal atoms as the medium for modulating the intensity profile of vector beams. A single metasurface is employed to generate both the control and signal vector beams, each with unique vectorial characteristics. The shaping of the signal beam profile is facilitated by the interaction with thermal atoms, which can be controlled by adjusting the control vector beam. This spatially selective absorption is a result of the thermal atoms' response to the varying polarizations within the vector beams. In this experiment, two distinct metasurface chips are fabricated to generate vector beams with doughnut-shaped and Gaussian-shaped intensity profiles. By adjusting the incident power and polarization state of the control light, the doughnut-shaped signal beams can be converted into a rotational dual-lobed pattern or the dimensions of the Gaussian-distributed signal beams can be modified. This study introduces a novel vector beam shaping technique by integrating metasurfaces with thermal atoms, offering significant promise for future applications requiring miniaturization, dynamic operation, and versatile control capabilities.

I. INTRODUCTION

Vector beams feature an inhomogeneous polarization distribution across their cross-section, offering enhanced flexibility for the spatial manipulation and control of light fields [1, 2]. This characteristic enables their widespread use in various applications, including optical manipulations [3–6], optical communications [7–9], and sensing technologies [10, 11]. Vector beams are conventionally generated through the use of wave plates, spatial light modulators, or digital micromirror devices. Although these approaches facilitate the manipulation of light fields, they also impose certain constraints and augment system complexity. In recent years, metasurface technology has made considerable progress, greatly improving the ability to manipulate light, especially in the field of shaping vector beams. Advanced micro-nano fabrication techniques have enabled the creation of nanoscale meta-atoms in metasurfaces, thereby allowing for precise manipulation of the polarization and intensity distributions of vector beams [12–16]. The application of metasurfaces in vector beam manipulation presents significant potential for advancements in optical tweezers [17] and image processing [18–20]. To facilitate the dynamic modulation of vector beams and enhance their manipulation, thereby enabling the investigation of diverse physical phenomena and broadening their potential applications, it is imperative to implement innovative control mechanisms. Recent advancements have demonstrated that exploiting light-atom interactions presents a promising approach for the control

of vector beams.

In the context of light-atom interactions, the state of atoms is altered by light, while simultaneously, atoms modify their properties in response to the light. This process involves transitions between different atomic energy levels through the absorption or emission of photons, with the probability of these transitions being governed by selection rules. Generally, the atomic response exhibits heightened sensitivity to the polarization state of the incident light. Variations in polarization states result in distinct atomic responses, thereby imparting a pronounced polarization dependence to the absorption process. Consequently, the utilization of atomic responses to vector beams has garnered extensive investigation across various domains, including magnetic field sensing [21–23], optical spatial mode extraction [24] and optical storage [25]. Nevertheless, in the present scenario of vector beam-atom interactions, vector beams are predominantly produced with traditional optical elements, which restricts the diversity of vector beams configurations that can be achieved.

Additionally, directly manipulating input signal parameters to control vector beams may disrupt the stability of the optical path. Therefore, incorporating additional physical fields to modulate the signal light proves to be significantly more effective. This modulation can be achieved by interacting with atoms using magnetic fields [26–28], electric fields [29], or light fields [30]. Among various methodologies, the use of a light field to shape another light field is particularly noteworthy due to its exceptional efficiency, simplicity, and minimal noise. This approach offers significant advantages over

the generation of magnetic and electrical fields, as well as the complexities associated with assembling experimental setups.

In this paper, we propose a metasurface capable of generating vector beams that exhibit a variety of polarization states along their beam profiles. A vectorial dual-beam configuration has been developed, consisting of control and signal beams that propagate concurrently in the same direction through the metasurface chip. By incorporating a thermal atomic vapor cell into the setup, a system is established where the vectorial dual-beam engages with an atomic ensemble, allowing for precise manipulation of the signal beam's intensity distribution. In this arrangement, the incident signal light remains unchanged, and the output signal beam's intensity profile is modulated by varying the power or polarization state of the control light. This facilitates a system where the signal beam is shaped or tailored by the control beam. In the experiment, we designed and fabricated two metasurface chips capable of generating vector beams with

distinct polarizations and intensity distributions. These chips were incorporated into the system to demonstrate its capability in regulating various vector beams configurations. Our approach capitalizes on the distinctive sensitivity of thermal atoms to vector beams, enabling flexible, low-noise, and highly efficient manipulation of the vector beams.

II. THEORY

Vector beams display an inhomogeneous polarization distribution across their cross-section. Metasurfaces enhance the generation versatility of vector beams by meticulously designing the geometry and arrangement of meta-atoms. When an input beam with a polarization state $|s_{\text{in}}\rangle$ passes through a meta-atom, it can result in an output beam with a polarization state $|s_{\text{out}}\rangle$, where $|s_{\text{in}}\rangle = \mathbb{J} |s_{\text{out}}\rangle$. In this context, \mathbb{J} denotes the Jones matrix associated with the meta-atom, as defined by [31]

$$\mathbb{J} = e^{i\psi_D} \begin{bmatrix} \cos\left(\frac{\psi_B}{2}\right) + i \sin\left(\frac{\psi_B}{2}\right) \cos(2\psi_R) & i \sin\left(\frac{\psi_B}{2}\right) \sin(2\psi_R) \\ i \sin\left(\frac{\psi_B}{2}\right) \sin(2\psi_R) & \cos\left(\frac{\psi_B}{2}\right) - i \sin\left(\frac{\psi_B}{2}\right) \cos(2\psi_R) \end{bmatrix}, \quad (1)$$

where ψ_D denotes the dynamic phase introduced, ψ_B signifies the birefringent phase difference between the two eigen-polarizations, ψ_R represents the orientation angle of the meta-atom. By fine-tuning the three parameters of the meta-atom, it is possible to produce various polarization states in the output light, even when the incident light has a fixed polarization. Consequently, by arranging the meta-atoms to create spatially varying distributions of $\{\psi_D, \psi_B, \psi_R\}$, the transformation from scalar beams to vector beams can be effectively achieved. Additionally, incorporating the geometric phase into the transformation process allows for the creation of vector beams that exhibit distinct polarization profiles corresponding to various input polarization states.

As illustrated in Fig. 1a, the incident light is an elliptically polarized Gaussian beam that passes through a metasurface chip. Consequently, the polarization profile of the resulting vector beams can simultaneously encompass various elliptically polarized fields. Further modifications to the input polarization state result in changes to the polarization profiles of the generated beams, as illustrated by transformations between Fig. 1a.I,II to Fig. 1a.III,IV. The distribution of polarization states can be represented by the Poincaré spheres

depicted in Fig. 1a.III,IV. Utilizing the designed metasurface, vector beams can be generated and modified by adjusting the polarization state of the input light. However, for a given metasurface structure, the output profile remains fixed for each specific polarized input light. In specific practical scenarios, there may be a need to modify or dynamically adjust the generated vector beams based on a particular input light. To address this necessity, we introduce an atomic ensemble and harness the mediating role of atoms to shape the signal beam using a control beam.

In Fig. 1b, a three-level hyperfine structure of an atom is illustrated, consisting of the ground state $|g\rangle$ and two excited states $|e\rangle$ and $|f\rangle$. Each state has several degenerate magnetic states, indicated by $|F_g, m_g\rangle$, $|F_e, m_e\rangle$, and $|F_f, m_f\rangle$, respectively. In this notation, $\{F_g, F_e, F_f\}$ signify magnitudes of the total atomic angular momentum, while $\{m_g, m_e, m_f\}$ represent the corresponding magnetic quantum numbers. When light interacts with an atom, an electron absorbs a photon and transitions from the ground state to an excited state within the atom. According to the selection rules, $|F_g, m_g\rangle \rightarrow |F_{e,f}, m_{e,f} = m_g - 1\rangle$ transition occurs for left-circularly polarized light (σ^-), and $|F_g, m_g\rangle \rightarrow |F_{e,f}, m_{e,f} = m_g + 1\rangle$ transition occurs for right-circularly

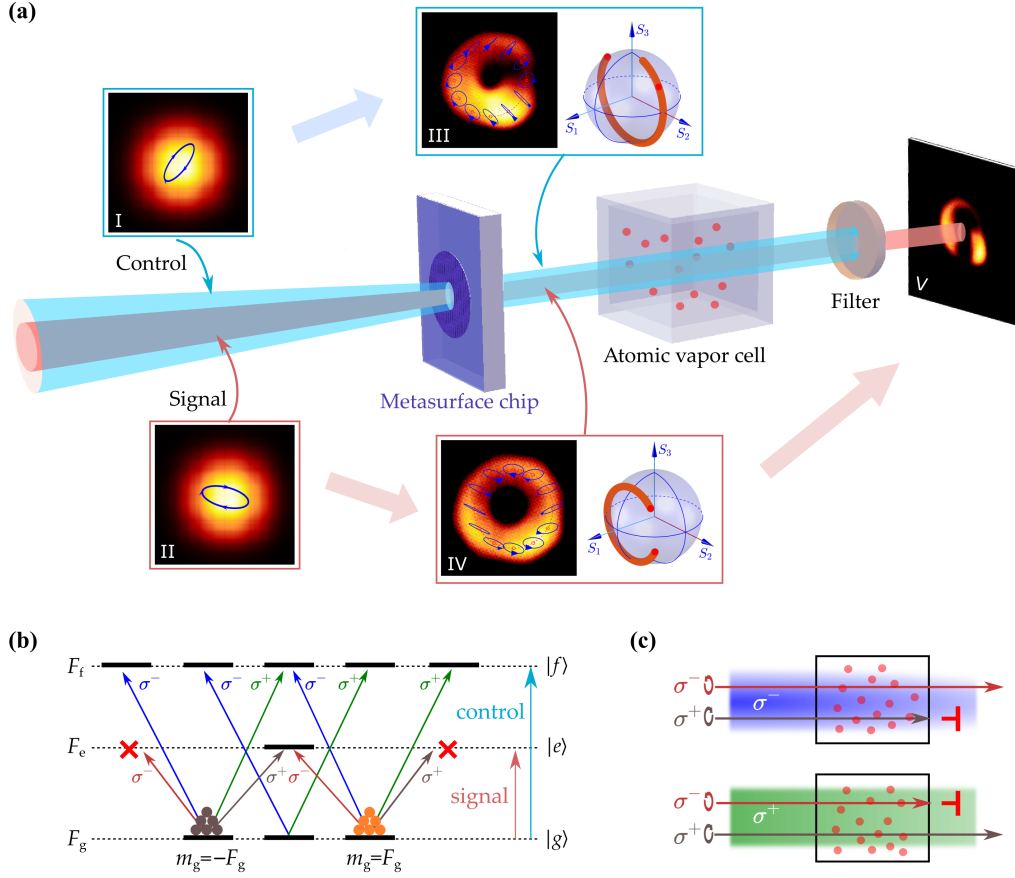


Figure 1. (a) The schematic diagram illustrates intensity modulation in vectorial dual beams produced by combining a single metasurface chip with a thermal atomic vapor cell. Both the input control light (I) and the signal light (II) are Gaussian beams, each displaying unique elliptical polarizations. The corresponding vectorial dual beams (III, IV) generated by the same metasurface exhibit their polarization states on the Poincaré sphere. The intensity profile of the output signal beam (V) is clipped due to interactions with thermal atoms. (b) The schematic illustrates the atomic energy levels and transitions facilitated by interactions with control and signal lights. The atomic transition $|g\rangle \rightarrow |f\rangle$ is induced by interaction with σ^- (σ^+) polarized control light. This redistributes the atomic population among ground magnetic states, enabling a forbidden transition $|g\rangle \rightarrow |e\rangle$ for σ^- (σ^+) polarized signal light, resulting in circular dichroism within the system. (c) The absorption of the signal beam by atoms is dependent on optical spin when influenced by control light. Specifically, when the control light is σ^- (σ^+) polarized, the signal light with σ^+ (σ^-) polarization is absorbed, whereas the signal light with σ^- (σ^+) polarization remains transparent.

polarized light (σ^+). A circularly polarized strong light resonant with the transition from $|g\rangle$ to $|f\rangle$, serving as the control light, induces a redistribution of the population among the atomic magnetic states within an ensemble. As the system approaches steady state, the majority of atoms occupy the $|F_g, m_g = -F_g\rangle$ for σ^- polarized light, and $|F_g, m_g = F_g\rangle$ for σ^+ polarized light.

At this point, a circularly polarized weak light, designated as the signal light and nearly resonant with the $|g\rangle \rightarrow |e\rangle$ transition, is introduced into the system. The polarization state of control light modulates the

population distribution among ground magnetic states, consequently influencing the absorption of signal light by atoms. When the control light is σ^+ polarized as shown in Fig. 1b, nearly all atoms are found in the $|F_g, m_g = F_g\rangle$. Consequently, the signal light with the same σ^+ polarization remains transparent due to the lack of available transitions. In contrast, the σ^- polarized signal light experiences significant absorption. Conversely, for σ^+ polarized control light, the effects on the signal lights are reversed. Consequently, when the control light interacts with an atomic ensemble, pro-

nounced circular dichroism is exhibited for weak signal light, as shown in Fig. 1c. This interaction leads to a differential absorption effect, where the atomic vapor interacts differently with the left-handed and right-handed circularly polarized components of the vector beams, resulting in the spatially varying absorption patterns within the beam profiles. The design of metasurface chips plays a pivotal role in generating vector beams with tailored polarization states, facilitating tunable atomic absorption and thereby enhancing the versatility of light field manipulation. Within this setup, a vectorial control beam can manipulate another vectorial signal beam, thereby enabling the spatial modulation of light intensity.

When vector beams passing through metasurface chip and entering in an atomic ensemble, the electric fields of the signal beam \mathbf{E}_s and the control beam \mathbf{E}_c , based on the atomic circular eigen-responses, are decomposed as in the cylindrical coordinate

$$\begin{aligned} \mathbf{E}_s(r, \phi) &= A_s(r, \phi) [a_-(r, \phi)\hat{\mathbf{e}}_- + a_+(r, \phi)\hat{\mathbf{e}}_+] \\ \mathbf{E}_c(r, \phi) &= A_c(r, \phi) [b_-(r, \phi)\hat{\mathbf{e}}_- + b_+(r, \phi)\hat{\mathbf{e}}_+] \end{aligned} \quad (2)$$

where $A_{s(c)}$ are the amplitude of signal (control) beams, and $a_{\pm}(b_{\pm})$ are the corresponding normalized components in the right (left) circularly polarized bases of $\hat{\mathbf{e}}_+$ ($\hat{\mathbf{e}}_-$). In scenarios where both the control and signal lights are vector beams traversing an atomic vapor cell, their interaction exhibits spatial variability due to non-uniform polarization distributions within the atomic ensemble. In regions where both the controlling and signal fields demonstrate circular polarization, the transmissivity of the signal light varies depending on whether their optical spins are antiparallel or parallel. Significant absorption of the signal light is observed when the control and signal fields possess opposite circular polarizations. Conversely, transparency prevails when they share the same circular polarization. Generally, when two beams are either elliptically or linearly polarized, they can be decomposed into left- and right-circularly polarized components. This decomposition leads to varying degrees of absorption for the signal light. Consequently, the output intensity of the signal light strongly depends on the spatial polarization distributions of both the signal and control beams. As shown in Fig. 1a.V, the output intensity of signal light (I_{out}) can be evaluated by

$$I_{\text{out}}(r, \phi) \propto A_s^2 \exp \left[-\frac{2\pi\kappa l}{\lambda_s} (1 - \mathbf{S}_s \cdot \mathbf{S}_c) \right], \quad (3)$$

where λ_s is the vacuum wavelength of signal light, κ corresponds to the maximal absorption coefficient for

signal and control fields with opposite circular polarizations, l is the length of light-atom interaction, \mathbf{S}_s (\mathbf{S}_c) denotes the average photon spin of signal (control) light, whose magnitude can be given by $S_s = a_+^2 - a_-^2$ and $S_c = b_+^2 - b_-^2$, respectively. The detailed derivations are provided in the Supplementary Materials.

III. EXPERIMENT AND RESULT

In this study, we engineered meta-atoms for a metasurface to modulate the parameters $\{\psi_D, \psi_B, \psi_R\}$ within the Jones matrix [31, 32]. By integrating the geometric phase effect, we generated vector beams exhibiting diverse linear and elliptical polarization profiles, tailored to various polarization states of input light. As shown in Fig. 2a, the metasurface pattern was fabricated on a 1-mm thick silicon-on-glass substrate and arranged in a circular configuration with a diameter of 0.5 mm. To achieve spatially varied polarization profiles for the output beams, we segmented the metasurface pattern into eight fan-shaped sectors. Each sector contains meta-atoms of a specific design, all sharing the same dimensions. Meta-atoms are constructed from silicon nanofins, each with a height (H) of 400 nm, dimensions that vary in length (L) and width (W) from 110 nm to 240 nm. These nanofins are arranged in a square array with a pitch (P) of 400 nm and oriented at angles ψ_R ranging from 0° to 360° according to design requirements. In the experiment, two distinct metasurfaces were meticulously designed as illustrated in Fig. 2b. By employing a variety of nanofin configurations, it was possible to achieve different sets of $\{\psi_D, \psi_B, \psi_R\}$, thereby facilitating the generation of vector beams with diverse polarization distributions. In Figs. 2c-d, the symbols at each azimuth angle (ϕ) represent a unique configuration $\{\psi_D, \psi_B, \psi_R\}$ employed for an individual sector. The eight sectors incorporate diverse silicon nanofin dimensions and arrangements (see the Supplementary Materials), generating vector beams with various polarization profiles for different input light polarization states.

In the experiment, an atomic ensemble was realized using a vapor cell containing rubidium (Rb) atoms. Referring to the level structure shown in Fig. 1b, we employed ^{87}Rb atoms and selected the $F_g = 2 \rightarrow F_f = 3$ transition of the D2 line as the $|g\rangle \rightarrow |f\rangle$ transition, as well as the $F_g = 2 \rightarrow F_e = 1$ transition of the D1 line as the $|g\rangle \rightarrow |e\rangle$ transition (see the Supplementary Materials). In practical scenarios, when atoms transition from excited states back to the ground state, some of them might undergo de-excitation to the $5^2S_{1/2}(F = 1)$ energy level, thereby exiting the three-level transition cycles under consideration. To address this issue, we intro-

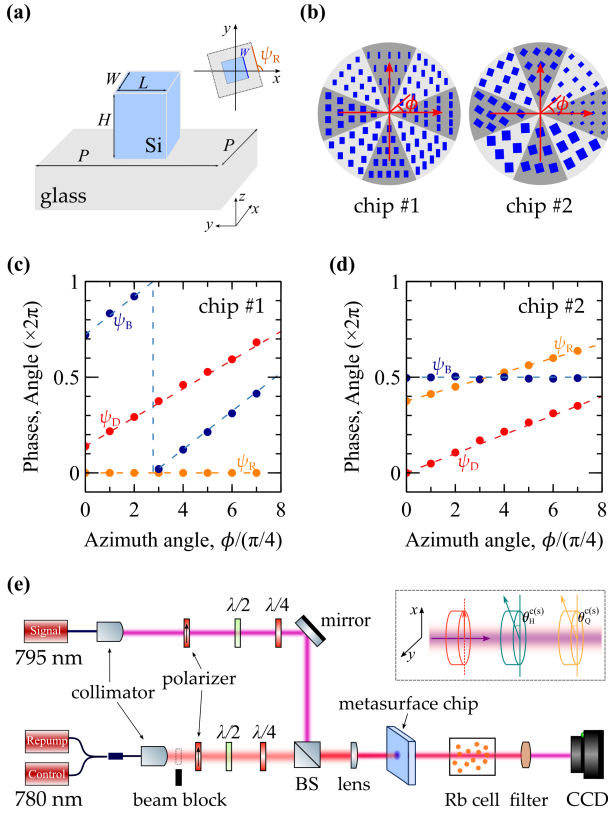


Figure 2. (a) Schematic of the metasurface’s meta-atom composed of silicon nanofins on glass substrate, featuring the nanofins with length L , width W , height H , and period P . The inset shows the rotation of a nanofin at an angle ψ_R . (b) Configuration of meta-atom in two metasurfaces chips (#1, #2) to generate different distribution of vector beam. For each azimuth angle (ϕ), a unique set of angles $\{\psi_D, \psi_B, \psi_R\}$ is used in individual sectors for (c) chip #1 and (d) chip #2. (e) Experimental setup with control/repump (red) and signal (pink) light beams. It includes wave plates for regulating polarized light, with an inset diagram showing the rotation angle of each wave plate. A beam splitter (BS) combines the beams, which then pass through a metasurface chip and a Rb vapor cell. A 795 nm narrow bandpass filter is utilized to ensure that solely the signal light is transmitted to a CCD camera.

duced a repump light that resonates with the $F = 1 \rightarrow F_f = 3$ transition of the D2 line. This ensures that the atoms are re-excited and returned to the relevant transition cycles.

The experimental system, as illustrated in Fig. 2e, was constructed based on a metasurface chip and an atomic Rb vapor cell to demonstrate the modulation of vector beams. The system includes a 795 nm laser for the signal light and two 780 nm lasers serving as the control and repump lights. The control and repump lights are merged

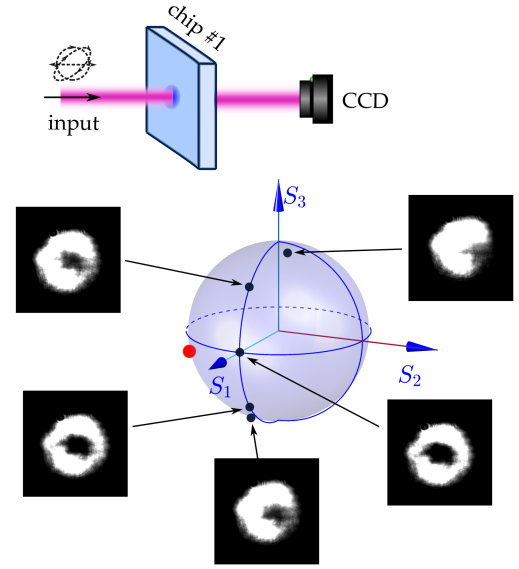


Figure 3. Intensity distribution of the signal vector beam generated by metasurface chip #1 varies with changes in the polarization state of the incident light, as represented on a Poincaré sphere.

into a single path using a 50 : 50 fiber coupler, subsequently converted into a free-space beam via a fiber collimator. The polarization state of the incident light is tuned by a combination of a polarizer, half-wave ($\lambda/2$) plate, and quarter-wave ($\lambda/4$) plate. As illustrated in the inset of Fig. 2e, the signal (control) light is initially polarized along the x -axis by the polarizer. Subsequently, to alter the polarization states, the $\lambda/2$ plate is aligned at angles θ_H^S (θ_H^C) and the $\lambda/4$ plate is positioned at angles θ_Q^S (θ_Q^C) relative to the polarizer. The signal light is combined with the control light via a beam splitter. Upon optimizing the spot size via a lens, the signal, control, and repump lights are concurrently transmitted across the metasurface chip. By adjusting the incident laser power, we facilitate the population of atoms in their ground state by the control and repump lights, meticulously avoiding saturation absorption. In the experiment, The side length of the cubic vapor cell is 20 mm, and to enhance the atomic vapor density, the temperature of the cell was maintained at 75°C. At the endpoint of the optical paths, a 795 nm narrow bandpass filter is implemented to block 780 nm lights, thereby precluding interference from control and repump beams on the final output. As a result, the signal light proceeds to enter a CCD camera to acquire intensity image of the signal beam.

With the specifically designed metasurface chip, the shape of the light beam can be adjusted by tuning the

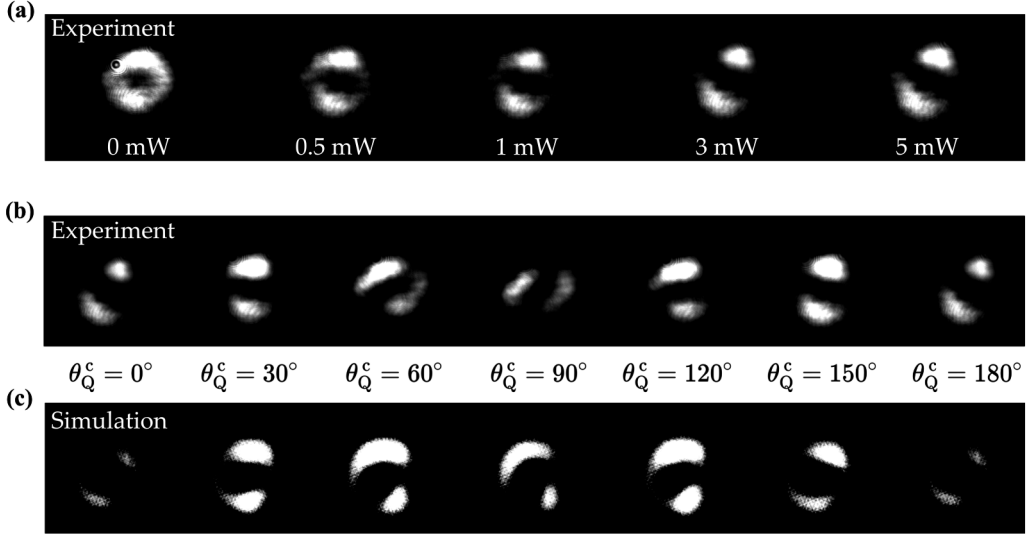


Figure 4. Experimental and simulation results of the intensity distribution for the signal vector beam modulated by the control vector beam, generated using chip #1. (a) Intensity distribution of the signal vector beam while varying the power of the control incident light from 0 mW to 5 mW. (b) The experimental and (c) simulated results for the intensity distribution of the signal beam with θ_Q^c on the control light varying from 0° to 180° , respectively. In the experiment, the powers of signal, control and repump lights are set as 0.04 mW, 5.5 mW and 1 mW, respectively.

polarization of the input light. As illustrated in the inset of Fig. 3, the Gaussian-distributed signal beam passes through chip #1 with varying polarization states (without control light). The output intensity patterns are illustrated in Fig. 3 for the respective input polarization states indicated on a Poincaré sphere. The capability to modulate the intensity distribution of the output signal beam is effectively demonstrated through the sole adjustment of the input signal light's polarization. However, the output beams are in forms of doughnut or crescent shapes, even for all the other input polarization states. Herein, we demonstrate that the signal beams can be further tailored by incorporating a control beam. To elucidate this manipulation, we maintain a constant power of $40 \mu\text{W}$ and a specific polarization state of the input signal light, as depicted by a red circular marker on the Poincaré sphere in Fig. 3. This configuration yields a doughnut-shaped output intensity distribution when utilizing chip #1. Subsequently, the control light is introduced to further tailor the signal beam's profile. Figure 4a illustrates the intensity distribution of the signal beam as a function of the varying incident power from 0 mW to 5 mW of the control light, with its polarization states set by $\{\theta_H^c, \theta_Q^c\} = \{20^\circ, 0^\circ\}$. Upon introducing the control light into the system and gradually increasing its incident power, the doughnut-shaped signal beam bifurcates into two lobes due to in-

homogeneous absorption induced by the atomic vapor. The observed inhomogeneity is attributed to the circular dichroism that arises from the interaction of atoms with the distinct vector beams of signal and control light, which are generated by the metasurface chip.

Indeed, adjusting the incident polarization of the control beam permits enhanced flexibility in sculpting the intensity profile of the signal beam. In the experiment, the power of the control light was set at 5.5 mW, with its polarization settings configured as $\theta_H^c = 20^\circ$ and θ_Q^c varied from 0° to 180° . The intensity distribution of the modulated signal beam is depicted in Fig. 4b, where the two distinct lobed shapes rotate due to varying polarizations of the control light. The intensity pattern of the signal beam rotates counterclockwise as θ_Q^c varies from 0° to 90° and clockwise as it ranges from 90° to 180° . The observed variation is directly attributable to the control vector beam's modulation of atomic absorption across various incident polarization states. The simulated results, obtained using equation (3), are illustrated in Fig. 4c and exhibit a satisfactory correspondence with the experimental findings.

Moreover, utilizing chip #2 and fine-tuning the polarization state of the incoming signal light, we produce a beam whose intensity distribution closely approximates a Gaussian profile, as depicted in the first pattern of Fig. 5a. Upon activation of the control light,

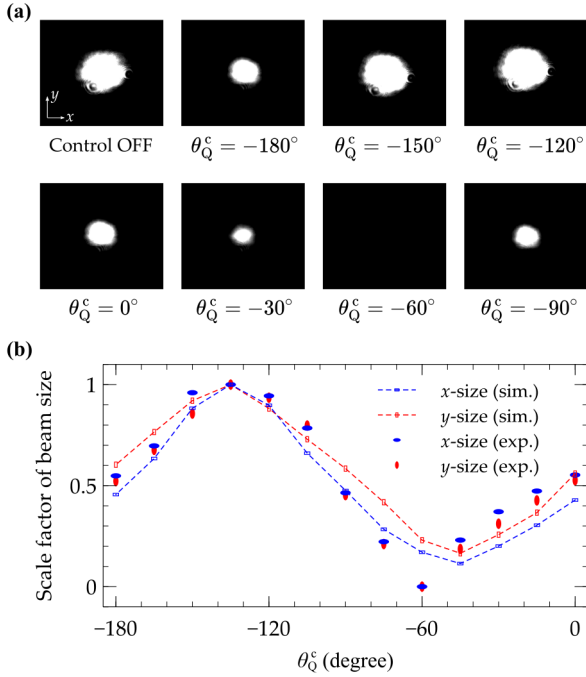


Figure 5. (a) Experimental results of intensity distribution for signal beam modulated by control light, with $\theta_H^c = 0^\circ$ and θ_Q^c varying from 0° to -180° , under chip #2. (b) Experimental and simulation results of scale factor of beam size versus θ_Q^c for the control light. The blue (red) ellipse symbol represents the beam size along the x -axis (y -axis) in the experimental results, while the blue (red) dashed line with a bar signifies the beam size along the x -axis (y -axis) in the simulation results.

with $\theta_H^c = 0^\circ$ and θ_Q^c varying from 0° to -180° , the beam size of the Gaussian-distributed signal beams can be adjusted in response to changes in the control polarization state. Figure 4b presents the scale factor of the beam size along both the x - and y -axes, comparing experimental data with calculated results (also see the Supplementary materials). It is clear that as θ_Q^c of the control light varies from 0° to -180° , the beam size can be altered by nearly an order of magnitude. This suggests that the shape of the signal beam is significantly influenced and tailored by the control vector beam through the thermal atomic vapor system. The discrepancies observed between the experimental and simulated results of θ_Q^c ranging from -60° to 0° are primarily attributed to deviations from the design specifications due to fabrication imperfections. The absence of a visible spot for $\theta_Q^c = -60^\circ$ as depicted in Fig. 5a is a consequence of the fixed exposure settings of the CCD camera.

IV. DISCUSSION

This study presents a system designed for vectorial dual-beam interactions with thermal atoms, specifically engineered for intensity clipping of vector beams. We utilize metasurface chips to generate dual vectorial beams: one as the control vector beam and the other as the signal vector beam. The vectorial dual-beam clipping method modulates the intensity of the signal vector beam without the need to adjust the parameters of the signal light itself. This method enhances both the robustness of the detection optical path and the modulation capabilities of vector beams.

In this study, we have developed two unique metasurface chip designs to demonstrate the generation and modulation of vector beams. However, the vector beams generated are not confined to these two designs alone. By precisely engineering metasurfaces with specific configurations of meta-atoms, a diverse distribution of light field outputs can be achieved. This flexibility empowers a multitude of applications through vector beam modulation, such as optical manipulations of micro-nano particles. Our experimental results reveal that the intensity distribution of the signal beam, when modulated by a control vector beam passing through two distinct metasurface chips, exhibits two characteristic patterns: a dual-lobed configuration and a Gaussian-like profile. The modulation of the polarization state of the control light facilitates the rotation of the dual lobes and the dynamic adjustment of the dimensions of the Gaussian-like profile, which in turn facilitates the efficient trapping and manipulation of micro-nano particles, even at the atomic level. Thus, this dynamic modulation technique possesses considerable potential for applications in atomic trapping, transportation, and associated fields. Furthermore, it also presents promising prospects in the realms of image processing and quantum information.

The metasurface is fabricated using micro-nano technologies; however, unavoidable manufacturing imperfections can introduce discrepancies between the actual structure and its intended design. As a result, these deviations may cause differences between the actual performance of the generated vector beams and theoretical predictions. Our simulations are predicated on ideal design parameters, which can lead to minor discrepancies between the theoretical predictions and the actual experimental results. In our simulations, the results are obtained using equation (3) which is derived from a phenomenological model (further details are provided in the Supplementary Materials). However, this simple model inaccurately captures the intermediate states between two perfect circular polarizations, leading to less accurate predictions for these scenarios. The precise methodology outlined in the Supplementary Mate-

rials is derived from the general atom-light interaction process. Nevertheless, determining the spatially variant atomic-induced susceptibility for vector beams persists as a significant challenge, primarily due to the voluminous nature of the required computations.

V. CONCLUSION

This study introduces a novel hybrid system that combines metasurfaces with thermal atomic vapor to precisely modulate vector beam intensity profiles. A vectorial dual-beam configuration is introduced, where both the control and signal beams are generated using a single metasurface chip. The inherent flexibility in the design of metasurfaces enables the generation of distinct vector beams through adjustment of their meta-atom arrangements and geometric configurations. By utilizing the absorption characteristics of atomic vapor, a medium with optical spin-dependent absorption is constructed, stemming from the control light modifying the atomic population distribution. The circular dichroism feature is utilized to effectively modulate the intensity distribution of the signal beam using the control beam. To demonstrate diverse modulation, we designed and fab-

ricated two metasurface chips capable of generating vector beams with various polarization distributions. By adjusting the power and polarization states of control light, we successfully tailored the intensity profiles of both doughnut-shaped and Gaussian-distributed signal beams. These advancements hold significant application prospects in particle trapping and manipulation, image processing, and quantum information.

Funding

This work is supported by the Fundamental Research Funds for the Central Universities under Grant KG21008401.

Disclosures. The authors declare no competing financial interests.

Data availability. Data underlying the results presented in this paper are not publicly available at this time but may be obtained from the authors upon reasonable request.

Supporting Information. Detailed theoretical derivation of the effective electric susceptibility of atomic vapor, experimental results of beam shaping, geometric parameters of meta-atoms, and simulated polarization distributions of vector beams.

-
- [1] Pattanayak, D. & Agrawal, G. Representation of vector electromagnetic beams. *Phys. Rev. A* **22**, 1159 (1980).
- [2] Hall, D. G. Vector-beam solutions of Maxwell's wave equation. *Opt. Lett.* **21**, 9–11 (1996).
- [3] Ma, J., Xie, Z. & Yuan, X. Tailoring arrays of optical stokes skyrmions in tightly focused beams. *Laser Photonics Rev.* 2401113 (2024).
- [4] Kumar, R. N., Nayak, J. K., Gupta, S. D., Ghosh, N. & Banerjee, A. Probing dual asymmetric transverse spin angular momentum in tightly focused vector beams in optical tweezers. *Laser Photonics Rev.* **18**, 2300189 (2024).
- [5] Donato, M. *et al.* Optical trapping of nanotubes with cylindrical vector beams. *Opt. Lett.* **37**, 3381–3383 (2012).
- [6] Kozawa, Y. & Sato, S. Optical trapping of micrometer-sized dielectric particles by cylindrical vector beams. *Opt. Express* **18**, 10828–10833 (2010).
- [7] Milione, G., Nguyen, T. A., Leach, J., Nolan, D. A. & Alfano, R. R. Using the nonseparability of vector beams to encode information for optical communication. *Opt. Lett.* **40**, 4887–4890 (2015).
- [8] Zhu, Z. *et al.* Compensation-free high-dimensional free-space optical communication using turbulence-resilient vector beams. *Nat. Commun.* **12**, 1666 (2021).
- [9] Zhao, Y. & Wang, J. High-base vector beam encoding/decoding for visible-light communications. *Opt. Lett.* **40**, 4843–4846 (2015).
- [10] Syubaev, S. *et al.* Plasmonic nanolenses produced by cylindrical vector beam printing for sensing applications. *Sci. Rep.* **9**, 19750 (2019).
- [11] Wu, H. *et al.* Cylindrical vector beam for vector magnetic field sensing based on magnetic fluid. *IEEE Photonics Technol. Lett.* **33**, 703–706 (2021).
- [12] Guo, Q. *et al.* Manipulation of vector beam polarization with geometric metasurfaces. *Opt. Express* **25**, 14300–14307 (2017).
- [13] Wen, D. *et al.* Broadband multichannel cylindrical vector beam generation by a single metasurface. *Laser Photonics Rev.* **16**, 2200206 (2022).
- [14] Zhang, C. *et al.* Optical metasurface generated vector beam for anticounterfeiting. *Phys. Rev. Appl.* **10**, 034028 (2018).
- [15] Fu, P. *et al.* Metasurface enabled on-chip generation and manipulation of vector beams from vertical cavity surface-emitting lasers. *Adv. Mater.* **35**, 2204286 (2023).
- [16] Cui, G. *et al.* Multifunctional all-dielectric quarter-wave plate metasurfaces for generating focused vector beams of bell-like states. *Proc. Spie.* **13**, 1631–1644 (2024).
- [17] Zhu, J.-L. *et al.* Multidimensional trapping by dual-focusing cylindrical vector beams with all-silicon metalens. *Photonics Res.* **10**, 1162–1169 (2022).
- [18] Kim, I. *et al.* Pixelated bifunctional metasurface-driven dynamic vectorial holographic color prints for photonic security platform. *Nat. Commun.* **12**, 3614 (2021).
- [19] Arbabi, A., Horie, Y., Bagheri, M. & Faraon, A. Dielec-

- tric metasurfaces for complete control of phase and polarization with subwavelength spatial resolution and high transmission. *Nat. Nanotechnol.* **10**, 937–943 (2015).
- [20] Deng, Z.-L. *et al.* Diatomic metasurface for vectorial holography. *Nano Lett.* **18**, 2885–2892 (2018).
- [21] Cai, G., Tian, K. & Wang, Z. Thermal atomic compass based on radially polarized beam. *Laser Photonics Rev.* 2400465 (2024).
- [22] Castellucci, F., Clark, T. W., Selyem, A., Wang, J. & Franke-Arnold, S. Atomic compass: detecting 3D magnetic field alignment with vector vortex light. *Phys. Rev. Lett.* **127**, 233202 (2021).
- [23] Qiu, S. *et al.* Visualization of magnetic fields with cylindrical vector beams in a warm atomic vapor. *Photonics Res.* **9**, 2325–2331 (2021).
- [24] Chang, H. *et al.* Atomic optical spatial mode extractor for vector beams based on polarization-dependent absorption. *Chin. Phys. B* **32**, 034207 (2023).
- [25] Ye, Y.-H., Dong, M.-X., Yu, Y.-C., Ding, D.-S. & Shi, B.-S. Experimental realization of optical storage of vector beams of light in warm atomic vapor. *Opt. Lett.* **44**, 1528–1531 (2019).
- [26] Yang, X. *et al.* Observing quantum coherence induced transparency of hybrid vector beams in atomic vapor. *Opt. Lett.* **44**, 2911–2914 (2019).
- [27] Sun, Y. & Wang, Z. Optically polarized selective transmission of a fractional vector vortex beam by the polarized atoms with external magnetic fields. *Opt. Express* **31**, 15409–15422 (2023).
- [28] Wang, J. *et al.* Measuring the optical concurrence of vector beams with an atomic-state interferometer. *Phys. Rev. Lett.* **132**, 193803 (2024).
- [29] Sedlacek, J. A. *et al.* Microwave electrometry with rydberg atoms in a vapour cell using bright atomic resonances. *Nat. Phys.* **8**, 819–824 (2012).
- [30] Hu, X.-X. *et al.* Noiseless photonic non-reciprocity via optically-induced magnetization. *Nat. Commun.* **12**, 2389 (2021).
- [31] Zhang, D., Feng, X. & Huang, Y. Orbital angular momentum induced by nonabsorbing optical elements through space-variant polarization-state manipulations. *Phys. Rev. A* **98**, 043845 (2018).
- [32] Cui, J., Qing, C., Feng, L. & Zhang, D. Exploiting the combined dynamic and geometric phases for optical vortex beam generation using metasurfaces. *arXiv* 2412.05121 (2024).